Journal of Materials Chemistry B

Accepted Manuscript

ROYAL SOCIETY OF CHEMISTRY

www.rsc.org/materialsB

Bioactive Saccharide-Conjugated Polypeptide Micelles for Acid-Triggered Doxorubicin Delivery

*Steven S.-S. Wang[2], Su-Chun How[2], Yun-Duan Chen[1], Ya-Hui Tsai[3], and Jeng-Shiung Jan[1]**

[1]Prof. J.-S. Jan, Yun-Duan Chen
Department of Chemical Engineering, National Cheng Kung University
No 1, University Rd., Tainan, 70101 Taiwan
E-mail: jsjan@mail.ncku.edu.tw

[2]Prof. Steven S.-S. Wang, Su-Chun How
Department of Chemical Engineering, National Taiwan University
No. 1, Sec. 4, Roosevelt Road, Taipei 10617, Taiwan
E-mail: sswang@ntu.edu.tw

[3]Dr. Y.-H. Tsai
Department of Surgery, Far Eastern Memorial Hospital
Pan-Chiao, New Taipei 220, Taiwan
E-mail: yahuitsai@gmail.com

Keywords: Glycopolypeptide, click chemistry, self-assembly, pH-responsive, biorecognition, drug delivery

Abstract

The synthesis and self-assembly of lactobionolactone-conjugated poly(L-glutamic acid)-*b*-poly(L-phenylalanine) amphiphilic polypeptides (Lac-PGA-*b*-PPhe) and their evaluation for anticancer drug doxorubicin (DOX) delivery have been investigated. Lactobionolactone was functionalized with azide group and successfully conjugated with the terminal alkyne groups on the polypeptides through click reaction and these amphiphilic glycopolypeptides self-assembled to form micelles with bioactive galactose units on the particle surface as confirmed by selective lectin binding experiments. Drug release experiments showed that DOX released faster from saccharide-conjugated micelles at acidic condition than at neutral condition. The DOX-loaded, saccharide-conjugated micelles exhibited a higher cytotoxicity toward HepG2 tumor cells than free DOX and saccharide-free micelles loaded with DOX at low concentrations, suggesting that the saccharide-conjugated micelles can effectively bind to the cells through specific recognition and subsequently the higher uptake of saccharide-conjugated micelles led to higher drug release and cytotoxicity under pH-sensitive condition.

1. Introduction

Amphiphilic block copolymers that are able to self-assemble into nano-sized structures including bilayers, micelles, and vesicles in selective solvents have been widely studied.[1, 2] Of them, polypeptide-based block copolymers have attracted growing attention due to their significance in basic research and their potential applications in biomedical field.[3-5] Polypeptides are biocompatible, biodegradable, and nontoxic since the building blocks are naturally occurring compounds in living systems. They possess essential structures and functions of proteins that can mimic the biological activities and supramolecular structures of natural proteins. Unlike the conventional polymers generally with a coil structure, polypeptides can adopt ordered conformation including α-helices and β-sheets. It has previously been demonstrated that the size and morphology of the self-assembled structures can be tuned by the chain conformation of polypeptide segments.[5, 6]

For applications in drug delivery system, the designed nanoparticles modified with active targeting groups have shown a significant enhancement of specifically accumulation at tumor site, due to molecular recognition to target cancer cells.[7, 8] Carbohydrates are found to play an important role in many biological events including cell-cell recognition, inflammation, immune response, and so forth.[9-11] Many efforts have been directed toward the synthesis of glycopolymers since they are an interesting alternative to glycoproteins. Despite the great advances in the synthesis of acrylate-based glycopolymers using controlled radical polymerization (CRP),[12] the development of polypeptide-based glycopolymers would be more desirable due to their higher resemblance to natural glycopeptides. Recent studies have demonstrated that well defined polypeptide-based glycopolymers, also known as glycopolypeptides, can be synthesized by ROP of protected glycomonomers or by postpolymerization modification strategies via click chemistry.[13-22] Click-type reactions are shown to be ideally effective for peptide glycosylation.[23, 24] Amphiphilic glycopolypeptides combining poly(γ-benzyl-L-glutamate) (PBLG) and oligosaccharides including hyaluronan

and dextran were successfully synthesized via Huisgen's click reaction.[14, 15] The functionalization of readily available carbohydrates on the side chains of polypeptides was also demonstrated by click-type reactions.[13, 16, 17, 19, 20, 22] Among these contributions, only a few studies have focused on synthesizing amphiphilic glycopolypeptides that can form self-assembled structures with bioactivity and these materials hold promise as drug carriers for targeted delivery.[13, 14, 20]

It would be desirable to develop glycopolypeptide drug carriers that not only can form self-assembled structures but also possess multiple functionalities such as targetability and stimuli-responsiveness. Our group has studied the synthesis and self-assembly of polypeptide-based block and graft copolymers.[25-31] These copolymers conjugated with bioactive saccharide group partially on the hydrophilic poly(L-lysine) (PLL) segments can self-assemble to form vesicles, which have been evaluated as targeted drug carriers.[26, 28] In this study, we propose to use Huisgen's click reaction for achieving saccharide conjugation of poly(L-glutamic acid)-*b*-poly(L-phenylalanine) (PGA-*b*-PPhe) amphiphilic polypeptides. The block polypeptides were synthesized by ring-opening polymerization (ROP) of γ-benzyl-L-glutamate (Bn-Glu) and L-phenylalanine (Phe) N-carboxyanhydrides using propargylamine as the initiator, followed by removing the protecting group. Lactobionolactone (Lac), a targeted ligand to liver cells,[8, 32] was functionalized with azide group and conjugated with the terminal alkyne groups of PGA-b-PPhe block copolypeptides through Huisgens cycloaddition.

The synthesis and self-assembly of Lac-conjugated PGA-*b*-PPhe (Lac-PGA-*b*-PPhe) were investigated through the use of light scattering (LS), electron microscopy, circular dichroism (CD), and aqueous electrophoresis. The Lac-PGA-*b*-PPhe amphiphilic glycopolypeptides were shown to self-assemble into micelles in aqueous solution and exhibited pH-responsiveness due to the presence of PGA. It is well known that simple polypeptides such as PLL and PGA are pH-sensitive polymers and have been incorporated in many pH-responsive drug carriers.[33] Selective lectin binding experiments were performed to confirm the successful

conjugation of the bioactive saccharide bearing galactose unit on the polypeptides. The Lac-conjugated micelles were employed for drug encapsulation and evaluated as targeted carriers for *in vitro* drug release. Previous study has demonstrated that the stimuli-responsive, galactose-conjugated particles can be uptaken more by the target hepatocyte cells as comparing with the non-stimuli-responsive particles and non-targed particles.[34] Hence it is expected that the as-prepared saccharidee-conjugated, pH-responsive micelles would be promising as drug carriers for targeted delivery. Moreover, these glycopolypeptides not only benefit from their biocompatible and biodegradable properties, but also can be costumed to possess different structures and functions of both carbohydrates and polypeptides for specific applications.[1, 17, 19, 20]

2. Materials and Methods

2.1. Materials

L-Glutamic acid γ-benzyl ester, L-Phenylalanine, lactobionic acid, Concanavalin A (Con A), and *Ricinus Communis* Agglutinin (RCA_{120}) lectin were purchased from Sigma-Aldrich, as well as propargylamine, triphosgene, anhydrous methanol and DMF (ACS Reagent). THF, dichloromethane, and diethyl ether (ACS Reagent, TEDIA) were dried by using Na metal (99.95%, in mineral oil). Hexane (ACS reagent, ECHO) was dried using calcium hydride (95%, Aldrich). Iodotrimethylsilane (Me3Sil, 97%, saturated with copper), doxorubicin hydrochloride (99.9%), and trifluoroacetic acid (TFA, 99%) were supplied by Alfa Aesar. Diisoproylethylamine (DIPEA) was purchased from Acros and used as received. All other chemicals were reagent grade and used as received.

2.2. Synthesis of lactobionolamidopropylazide (Lac-N_3)

Lactobionic acid was first converted to the corresponding lactobionolactone based on reported procedure.[35] Briefly, lactobionic acid (10 g) was dissolved in anhydrous methanol (100 mL) in the presence of TFA as a catalyst (10 mol% with respect to the lactobionic acid)

at 50 °C, followed by repeating the evaporation in vacuum several times. Then, lactobionolactone (9 g) and 3-azidopropylamine (4 g) were dissolved in methanol with catalytic amount of DIPEA at room temperature for 24 h, followed by removal of methanol. The product was purified by precipitation from chloroform and dried in vacuum.[35]

2.3. Synthesis of poly(γ-benzyl L-glutamate)-*block*-poly(L-phenylalanine) (PBLG-*b*-PPhe) block copolypeptides

The polypeptide synthesis was initiated by the propargylamine as an initiator to sequentially polymerize γ-benzyl-L-glutamate (Bn-Glu) and L-phenylalanine (Phe) NCAs by following reported procedure.[21, 36] DMF was used for the synthesis of poly(γ-benzyl L-Glutamate)-*block*-poly(L-Phenylalanine) (PBLG-b-PPhe) block copolypeptides with different molecular weights and block ratios at room temperature. Below a detailed description of the synthesis procedure is given for a specific diblock copolypeptide, $PBLG_{20}$-*b*-$PPhe_4$.

In the glove box, Bn-Glu NCA (1 g, 4.2 mmol) and propargylamine (1.2 mg, 0.21 mmol) were weighted out, placed in 100 mL flasks and removed from the glove box. Dry DMF (10 mL for Bn-Glu NCA and 1 mL for propargylamine) was transferred to the two flasks using a Schlenk line. The propargylamine solution was then transferred to the Bn-Glu NCA solution through a cannula under argon atmosphere. Immediately after addition of the propargylamine solution, the flask was stirred for 48 h. Phe NCA (0.14 g, 0.84 mmol) was weighted out, dissolved in (~ 5 mL) and added to the reaction mixture. After stirring for additional 120 h, the copolypeptide was isolated by adding diethyl ether containing 1 mM HCl to the reaction mixture, causing precipitation of the copolypeptides. The copolypeptides were dried in vacuum to give a white solid.

2.4. Synthesis of poly(L-glutamic acid)-*block*-poly(L-phenylalanine) (PGA-*b*-PPhe) block copolypeptides

The benzyl protecting groups were removed by using Me_3SiI (150 μL Me_3SiI/1 mmol Bn-Glu). The block copolypeptides were completely dissolved in anhydrous dichloromethane,

respectively, followed by adding Me_3SiI. All operation and reactions were done under an inert atmosphere. The reaction mixture was left to stir for 24 h at 40 ^oC in the dark, followed by adding hexane to precipitate the polypeptides. After removing hexane by evaporation, the basic water (pH ~ 12) was added to dissolve the polypeptides. Then the solution was dialyzed against DI water for 3 days using a cellulose membrane dialysis tube (Sigma, MWCO 12,000–14,000 g/mL) and freeze-dried to yield the product as a white sponge material.

2.5. Conjugation of saccharides

The conjugation of Lac-N_3 to the polypeptide micelles was carried out by copper-catalyzed azide-alkyne cycloaddition.[23, 24] Briefly, the polypeptides and Lac-N_3 (3 mmol/1 mmol alkyne) were dissolved in de-ionized (DI) water. To the solution, *tert*-butyl alcohol (*t*BuOH, 30 v/v%) was added. After adding $CuSO_4$ (0.05 mmol) and ascorbic acid sodium salt (0.5 mmol), the resultant solution was stirred at 40 ^oC for 3 days. The solvent was degassed before use. Then the solution was dialyzed against DI water for 3 days and the polymer was collected by freeze-drying. The conjugation efficiency of Lac-N_3 was determined by ^{1}H-NMR in D_2O.

2.6. Preparation of polymer micelles and critical micelle concentration (*cmc*) measurements

The micellar solution was first prepared by direct dissolving the polypeptides or glycopolypeptides in the solution of pH 12.0 at a concentration of 2 mg/mL and then sonicated for 10 min (pulse on for 5 sec and off for 5 sec). Then, the solution pH was adjusted to 7.4 using 0.1 M HCl.

Critical micelle concentrations (*cmc*) of Lac-PGA-*b*-PPhe amphiphilic glycopolypeptides were measured using fluorescence probe technique. Pyrene solution (1.0×10^{-5} M) in acetone was evaporated under nitrogen gas stream in a vial. The particle solution at pH 7.4 was added into the vial and the final concentration of pyrene was 1.0×10^{-7} M. After placing the resultant solutions in a refrigerator overnight, the solutions were taken

out from the refrigerator. Once the temperature of the solutions reaching the room temperature, the emission spectra were recorded with the wavelength between 350 and 500 nm at an integration time of 1.0 s using a fluorescence spectrophotometer (Hitachi FL-4500, Japan). The *cmc* values were determined from the change of the I_{385}/I_{372} value of pyrene since the emissions of pyrene at 372 and 385 nm wavelengths are sensitive to the surrounding environment.

2.7. Carbohydrate-lectin binding recognition

The lectin recognition activity of the micellar solution was determined by analyzing the change of the turbidity at 450 nm at room temperature. The RCA_{120} lectin solutin (1 mg/mL) was first prepared in 0.01 M phosphate buffered saline (PBS) at pH 7.4, followed by transferring the lectin solution into a cuvette for baseline measurements. The micellar solution (60 μL, 2 mg/mL) was added into the cuvette containing lectin solution (540 μL). The final polymer concentration was 0.2 mg/mL in the as-prepared lectin solution. The solutions were gently mixed using a pipet and the absorbance at 450 nm was recorded immediately. Con A as a control lectin was used under the same experimental conditions.

2.8. In vitro drug release

Doxorubicin (DOX) loading was prepared by dissolving 1 mg of doxorubicin hydrochloride in 5 mL of micelle solutions with 2 mg/mL of polypeptide concentration at pH 7.4, followed by sonication for 30 min. The excess drug was removed by centrifugation. Specifically, the solution was transferred to a Vivaspin 6 centrifugal concentrator filter unit with nominal molecular weight limit of 30 kDa (Sartorius, USA) and centrifuged at 6000 rpm for 5 min. The filtrate was taken out the filter unit and the DOX-loaded micelle solutions was diluted to 5 mL using DI water. The centrifugation proecess was repeated at least three times. Drug concentrations in the filtrate and the drug-loaded vesicle solution were analyzed by UV-vis spectroscopy at the wavelength of 485 nm with reference to a calibration curve. The DOX loading was quantified by giving loading capacity (LC, mass of DOX in vesicles/mass of

polymer). The DOX loading content was cross-checked by the following method. The absorbance of the filtrate at the wavelength of 485 nm was measured and quantified from the calibration curve of DOX in PBS. The amount of DOX encapsulated in the vesicles was quantified by subtracting the excess drug. Each experiment was performed in triplicate.

For the drug release experiments, the DOX-loaded micelle solutions (1 mL) were placed in a cellulose membrane dialysis tube (MWCO 6,000-8,000 g/mol) and dialyzed against 50 mL of PBS (pH 4.7 or 7.4, 0.15 N) at 37 ^{o}C with a shaking rate of 100 rpm. The DOX-loaded micelle solution was placed in an thermal bath with the temperature kept at 37 ^{o}C. The micelle solution was taken out at designated time intervals and measured by fluorescence spectrophotometry (Hitachi FL-4500, Japan) at excitation wavelength 480 nm to a calibration curve. Each experiment was performed in triplicate.

2.9. Instrument and characterization

Gel permeation chromatography (GPC) measurements were performed on a Viscotek system equipped with three detectors, which are RI (VE3580, Viscotek), right angle light scattering, and viscometer (Dual 270, Viscotek). Two ViscoGEL I-Series columns (catalog number: I-MBLMW-3078 and I-MBHMW-3078, Viscotek) for efficient separation, eluted with 0.1 M LiBr in DMF at 55 ^{o}C. Polystyrene standards were utilized for calibration. The elution flow rate was 1 mL/min. ^{1}H-NMR spectra were recorded on Bruker AV-500 spectrometers. Transmission electron microscopy (TEM) measurements were performed on a Hitachi H7500 microscope with a Tungsten lamp and an excitation voltage of 120 kV. The particle solution (10 μL) was placed on a carbon-coated copper grid and then negatively stained with uranyl acetate for 30 s and dried in air overnight before TEM characterization. The hydrodynamic diameter (size), polydispersity index (PDI), and zeta potential of the self-assembled structures were measured using Malvern Zetasizer, NANO ZS (Malvern Instruments Limited, UK) equipped with a He–Ne laser (4 mW, 633 nm). The size and PDI of the self-assembled structures were determined using Malvern Instruments Dynamic Light

Scattering software. The particle solutions were adjusted to desired pH value using NaOH or HCl solutions. Each data point was obtained from the samples prepared in three different batches for DLS and zeta potential measurements. FTIR spectra were recorded using a Thermo Nicolet Nexus 670 FTIR and 32 scans were collected at a spectral resolution of 1 cm^{-1}. Far-UV circular dichroism (far-UV CD) spectra of the samples were acquired over the wavelength range of 190-260 nm using a 0.1 cm quartz cell on a JASCO J-815 spectrometer (JASCO Inc, Japan).

2.10. MTT reduction assay

The ability of cells to reduce the metabolic dye MTT to a blue formazan product was taken as an indication of the cell viability. The cytotoxicity of micelle, free DOX, or DOX-loaded PGA_{20}-*b*-$PPhe_4$/Lac-PGA_{20}-*b*-$PPhe_4$ on HepG2 cells was examined by MTT reduction assay. The HepG2 cells were cultured onto a 96 well plate (1×10^5 cells/mL) using Dulbecco modified Eagle's medium (DMEM, Gibco) supplemented with 10% fetal bovine serum (FBS, Caisson) under a humidified atmosphere of 5% CO_2 at 37 ^oC. After culturing for 24 h, the medium was first replaced with the culture medium containing polypeptide or drug with designated concentration. Next, the viability of adherent cells was determined after culturing for another 24 h. By adding10 μL-5g/L 3-(4,5-dimethylthiazol-2-yl)-2,5-diphenyltetrazolium bromide (MTT) to the cells, the tetrazolium salt was converted into an insoluble purple formazan salt. After 4 h-incubation, dimethyl sulfoxide (DMSO) was added to dissolve the formed formazan salt. The absorbance at 570 nm of the resulting solution was measured using an ELISA plate reader (μQuant). The viability data were reported as the percentage of the MTT reduced by the cells treated with the samples relative to the MTT reduced by the untreated cells (control group).

2.11. Cellular uptake

The cellular uptake behavior of the DOX-loaded micelles was examined using flow cytometry. HepG2 cells (2×10^5 cells/mL) were seeded in 6 well culture plates and cultured

under a humidified atmosphere of 5% CO_2 at 37 ^oC for 24 h. The cells were then treated with free DOX, DOX-loaded PGA_{20}-b-$PPhe_4$, and DOX-loaded Lac-PGA_{20}-b-$PPhe_4$ for 1, 2, or 4 h (DOX concentration = 6 μg/mL) at pH 7.4. Thereafter, the cells were lifted/detached using triple express (GIBCO) and washed with PBS buffer. The DOX uptake was analyzed on a flow cytometry (Beckman Coulter FC500). A minimum of 1×10^4 cells was analyzed from each sample with the DOX fluorescence intensity. DOX fluorescence at the emission wavelength of 570 nm was recorded upon exciting at 488 nm.

Confocal laser scanning microscopy (CLSM, Leica TCS SP2 MP) was also used to observe the cellular uptake of the free DOX and DOX-loaded micelles. HepG2 and fibroblast L929 cells (2×10^5 cells/mL) were seeded onto round glass coverslips with a diameter of 22 mm, which were placed in 6 well plates, and cultured under a humidified atmosphere of 5% CO_2 at 37 ^oC overnight. The cells were treated with free DOX, and DOX-loaded PGA_{20}-b-$PPhe_4$, and DOX-loaded Lac-PGA_{20}-b-$PPhe_4$ for 1, 2, or 4 hr (DOX concentration = 6 μ g/mL). Then the cells were washed and fixed with 4% formaldehyde for half an hour. The coverslips were put on the glass microscopy slides and analyzed by CLSM. The DOX fluorescence was excited with a 488 nm argon blue laser, and the emission was collected through a 505–525 nm barrier filter. Finally, the samples were imaged using a 63× oil-immersion objective lens.

2.12. Statistical analysis

All data were presented as mean ± standard deviation (S.D.) from n independent determinations. Statistical analysis was made by performing Student's *t* test assuming unequal variances for n independent determinations, where the specific n values are reported in the figure legends. Unless otherwise noted, significance was determined as $p < 0.05$.

3. Results and Discussion

3.1. Synthesis and Characterization of Block Copolypeptides

The block copolypeptides, poly(γ-benzyl L-glutamate)-*b*-poly(L-phenylalanine), (PBLG-*b*-PPhe), were synthesized by sequential ROP of benzyl-L-glutamate and L-phenylalanine NCAs using propargylamine as the initiator (Scheme 1), in which the amino group of propargylamine could undergo a nucleophilic addition to the carboxyl group connected to α-carbon.[37] Table 1 summarises the block copolypeptide molecular weight and composition as determined by GPC and ^{1}H NMR. GPC measurements using DMF as the eluent were performed to characterize these copolypeptides (Figure S1). The GPC chromatograms exhibited unimodal peaks, implying that the successful synthesis of block copolypeptides. These block copolypeptides showed narrow molecular weight distributions, evidenced by the low M_w/M_n values (1.05~ 1.15). The block ratio can be tuned by varying the molar ratio between the BLG and Phe NCA monomers. Figure 1 shows the ^{1}H NMR spectra of the PBLG-*b*-PPhe block copolypeptides in CF_3COOD. All the chemical shifts can be assigned to the protons on the block copolypeptides and propargylamine. It is worth to note that the peak of the methylene protons ($CHCC\underline{H_2}NH_2$) in propargylamine appears at 4.1 ppm. The DP of each block and block ratio were calculated based on the integrated areas of the protons on polypeptides (-$COOC\underline{H_2}C_6H_5$, -$COOCH_2C_6\underline{H_5}$, and -$CHCH_2C_6\underline{H_5}$) and initiator ($CHCC\underline{H_2}NH_2$) (Figure 1). The calculated DPs from NMR were found to be reasonably comparable with those obtained from GPC.

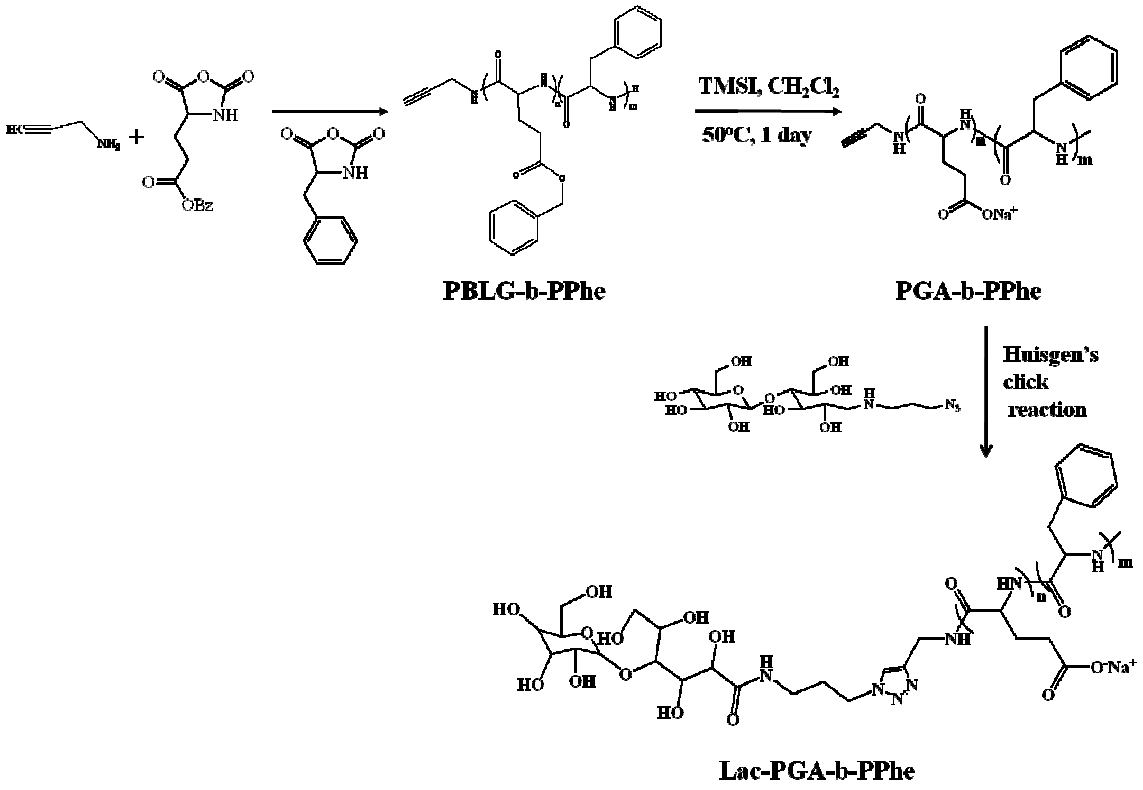

Scheme 1. Preparation of saccharide-conjugated polypeptides.

Table 1. Characterization of PBLG-*b*-PPhe block copolypeptides.

Sample code	Composition ratio[a] Initiator:BLG:Phe	M_n ($\times 10^3$)[b]	M_w/M_n[b]
$PBLG_{20}$-*b*-$PPhe_4$	1 : 20 : 4	7.6	1.11
$PBLG_{30}$-*b*-$PPhe_7$	1 : 30 : 7	10.4	1.10
$PBLG_{40}$-*b*-$PPhe_{14}$	1 : 40 : 14	11.7	1.07
$PBLG_{66}$-*b*-$PPhe_8$	1 : 66 : 8	19.5	1.08

[a]Determined by ^{1}H NMR. The molar ratio of propargylamine : BLG : Phe

[b]Measured by GPC.

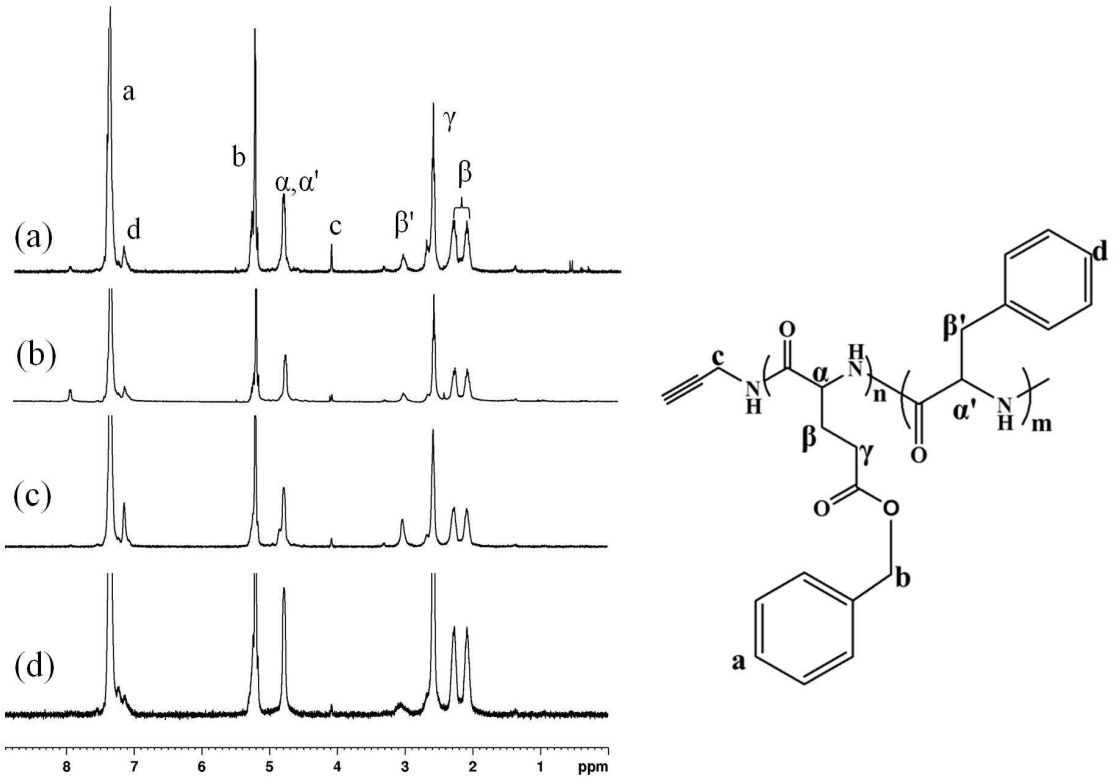

Fig. 1 ^{1}H NMR spectra of (a) $PBLG_{20}$-b-$PPhe_4$, (b) $PBLG_{30}$-b-$PPhe_7$, (c) $PBLG_{40}$-b-$PPhe_{14}$, and (d) $PBLG_{66}$-b-$PPhe_8$ block copolypeptides in CF_3COOD.

3.2. Formation of Polypeptide Assemblies

To attain the amphiphilic block copolypeptides, the benzyl groups in PBLG-*b*-PPhe block copolypeptides were removed by using Me_3SiI, as evidenced by elimination of peaks at 5.2 and 7.2 ppm in ^{1}H NMR (Figure 2). Two block copolypeptides, PGA_{20}-*b*-$PPhe_4$ and PGA_{40}-*b*-$PPhe_{14}$, were chosen for further saccharide conjugation and their self-assembly behavior in aqueous solution was investigated by TEM, DLS, aqueous electrophoresis, and CD. TEM characterization revealed that these PGA_{20}-*b*-$PPhe_4$ and PGA_{40}-*b*-$PPhe_{14}$ assemblies showed spherical micelle-like form (Figure 3a and c). As is known, the aggregate structure is strongly related to the weight fraction (f_{phil}) of hydrophilic blocks in the block copolymers.[38, 39] The weight fractions of hydrophilic blocks for PGA_{20}-*b*-$PPhe_4$ and PGA_{40}-*b*-$PPhe_{14}$ were found to

be about 80 and 70%, respectively. This strongly suggests that these amphiphilic copolypeptides can self-assemble into micellar structure. The particle sizes of these two micelles were measured to be 111.6 and 108.2 nm, respectively (Table 2). DLS measurements revealed that the autocorrelation function with a smooth baseline at higher decay time (> 1000 μs) (Figure S2). Since the counter length of the polypeptide chains are much smaller than 100 nm, the block copolypeptides possibly self-assembled to form compound micelles in which some heterogeneous domains formed by PGA chains were surrounded by the hydrophobic PPhe domains. The particle sizes determined by DLS analysis were consistent with those from TEM characterization. The size distributions were found to be relatively narrow (Figure S3), evidenced by the PDI values smaller than 0.25 (Table 2). In addition, the zeta potential values of these micelles indicated that they had a negative charged surface due to the presence of carboxyl group, indicating that the micelles can be well stabilized by the outer PGA chain.

Table 2. Hydrodynamic diameter (size), polydispersity index (PDI), critical micelle concentration (*cmc*), and zeta potential of polypeptide and glycopolypeptide assemblies.

Sample code	Size (nm)	PDI	*cmc* (mg/mL)	Zeta potential (mV)
PGA_{20}-*b*-$PPhe_4$	111.6 ± 12.3	0.22 ± 0.01	---	-38.2 ± 2.2
PGA_{40}-*b*-$PPhe_{14}$	108.2 ± 3.7	0.19 ± 0.01	---	-33.2 ± 1.3
Lac-PGA_{20}-*b*-$PPhe_4$	118.4 ± 8.5	0.21 ± 0.01	0.042	-24.7 ± 1.1
Lac-PGA_{40}-*b*-$PPhe_{14}$	114.8 ± 5.6	0.17 ± 0.01	0.021	-28.2 ± 1.8

3.3. Conjugation of Saccharides via Click Chemistry

Conjugation of cell-specific saccharide group onto the polypeptide assemblies can lead the as-prepared polypeptide micelles to be served as targeted drug carriers. Previous studies have

demonstrated that Cu(I)-catalyzed click chemistry can be employed to synthesize glycopolypeptides with high efficiency via clicking of sugar azides to the alkyne side chains of polypeptides.[15, 19, 20] In this study, the terminal alkyne groups on the polypeptides were conjugated with azide-functionalized saccharides via click chemistry. Lactobionolactone with a bioactive sugar moiety, galactose, is known to be a model targeted ligand to liver cells.[8, 28] The azide-functionalized lactobionolactone, lactobionolamidopropylazide (Lac-N_3), was first synthesized by the aminolysis of azidopropylamine and lactobionolactone. Lac-N_3 was then conjugated onto the terminal alkyne groups via Cu-catalyzed azide-alkyne cycloaddition (Scheme 1).[23, 24] FTIR spectrum of the Lac conjugated block copolymer confirmed the absence of the absorbance peak of azido and acetylene groups (Figure 2a) and ^{1}H NMR spectrum of Lac conjugated block copolymer showed the presence of the protons of saccharide (Figure 2b), indicating the successful conjugation of Lac on the polypeptides. As verified by TEM analysis, saccharide-conjugated PGA-*b*-PPhe block copolypeptides self-assembled to form micelles as well (Figure 3b and 3d). Small angle X-ray scattering (SAXS) measurements confirmed that the micellar morphology with their patterns well fitted by spherical block copolymer micelle model (Figure S3). DLS measurements revealed that after saccharide conjugation the particle sizes were found to be comparable with that of the parent micelles (Table 2 and Figure S4). The critical micelle concentrations (*cmc*) of Lac-PGA_{20}-*b*-$PPhe_4$ and Lac-PGA_{40}-*b*-$PPhe_{14}$ were measured to be 0.042 and 0.021 mg/mL, respectively. Zeta potential measurements revealed that the charge carried by the saccharide-conjugated micelles was lower than that carried by sugar free micelles, which can be attributed to the shielding of saccharide moiety.

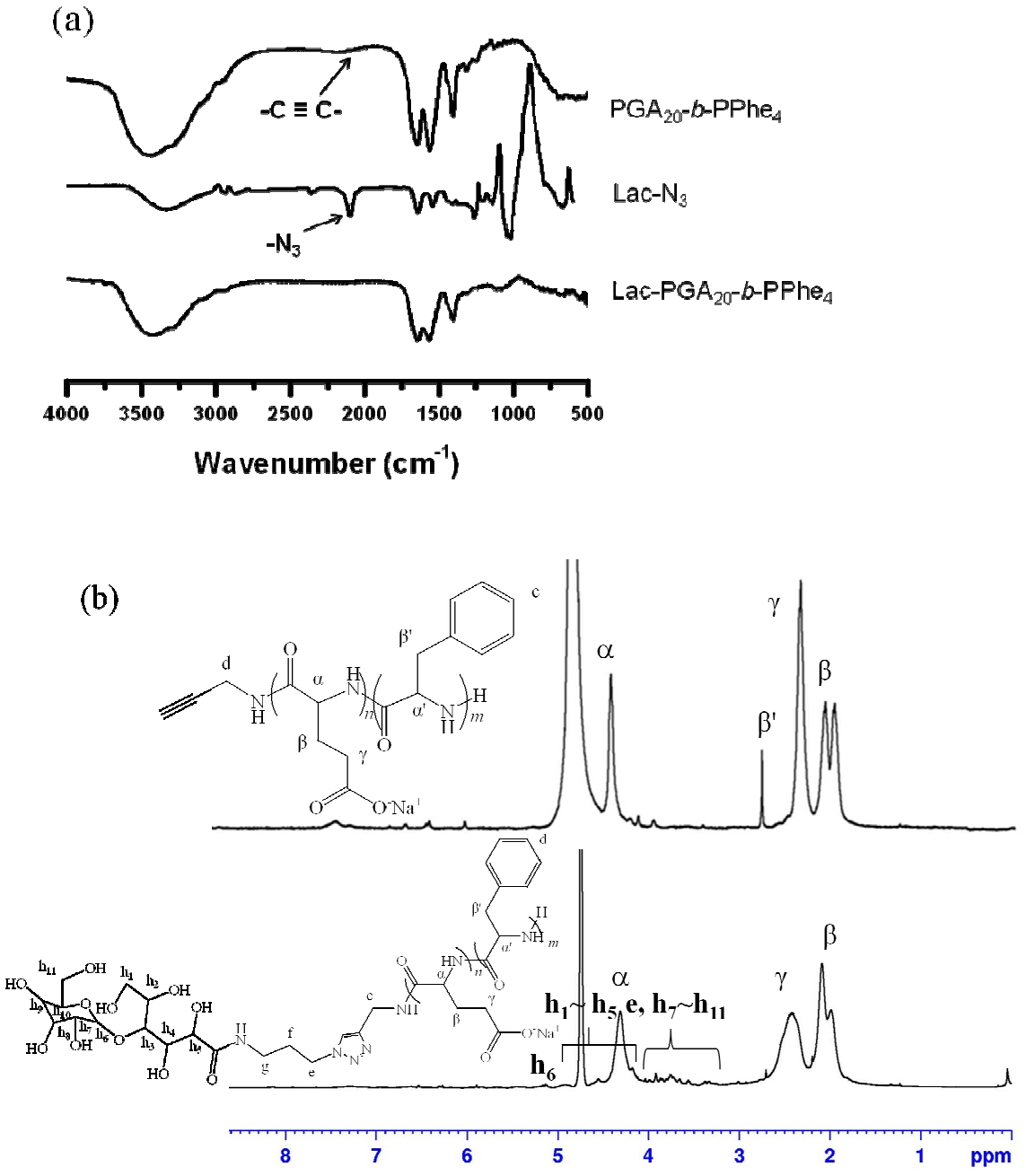

Fig. 2 (a) FTIR spectra of PGA_{20}-*b*-$PPhe_4$, Lac-N_3, and Lac-PGA_{20}-*b*-$PPhe_4$ and (b) ^{1}H NMR spectra of PGA_{40}-*b*-$PPhe_{14}$ and Lac-PGA_{40}-*b*-$PPhe_{14}$ in D_2O.

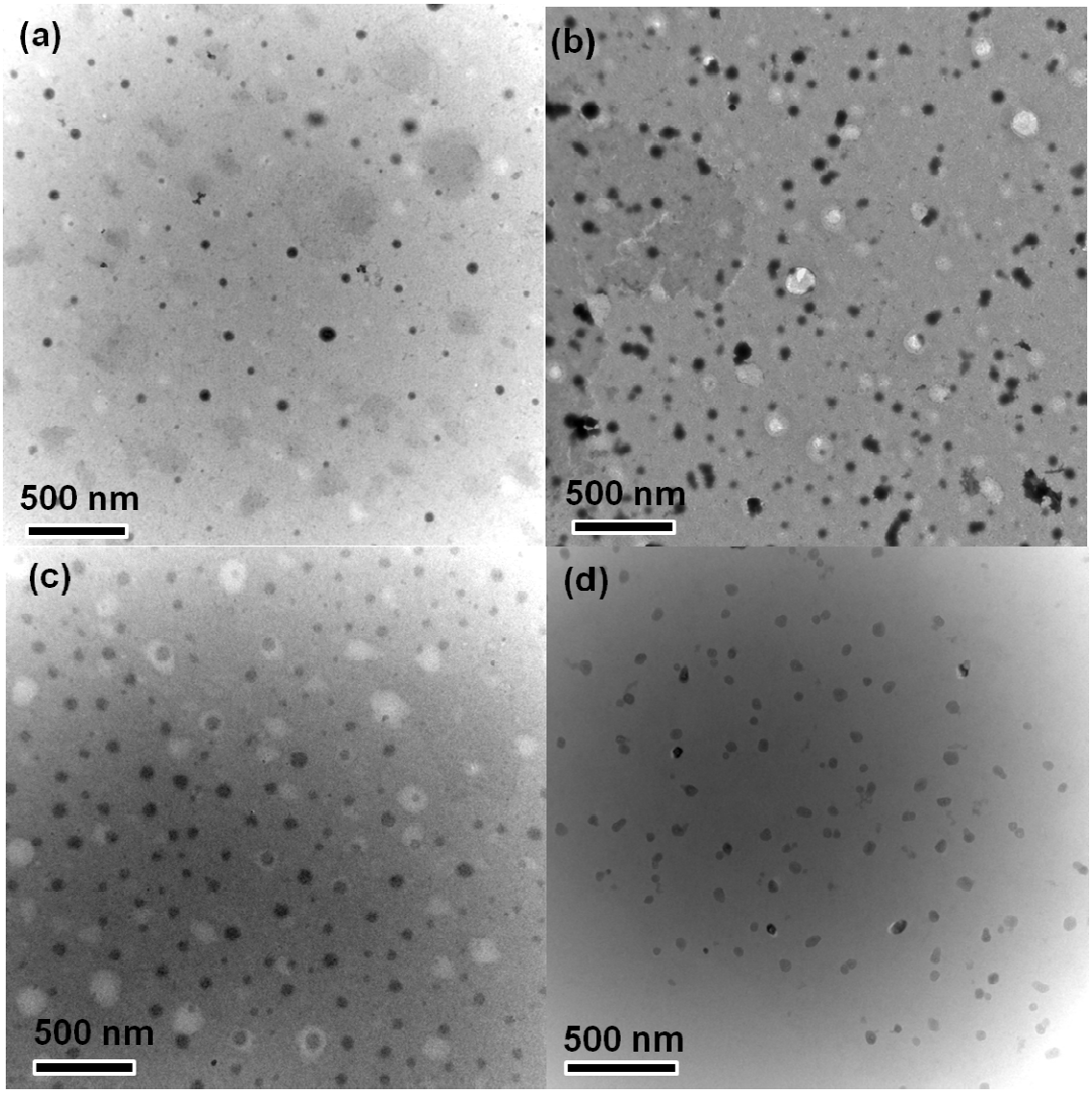

Fig. 3 TEM images of (a) PGA_{40}-*b*-$PPhe_{14}$, (b) Lac-PGA_{40}-*b*-$PPhe_{14}$, (c) PGA_{20}-*b*-$PPhe_4$, and (d) Lac-PGA_{20}-*b*-$PPhe_4$ micelles.

3.4. Bioactivity of Saccharide-Conjugated Micelles

Carbohydrates play an important role in biological recognition events mediated by highly specific and non-covalent carbohydrate-lectin interactions. The carbohydrate-lectin binding measurements were performed to evaluate the bioactivity of the saccharide-conjugated micelles, involving mixing the saccharide-conjugated micelles solution with a lectin that is selective for the sugar moiety. *Ricinus communis* Agglutinin (RCA_{120}) is a known specific lectin for the selective binding of galactosyl residues.[40] Previously, the sugar-containing

polymersomes formed by self-assembly of poly(benzyl L-glutamate)-*b*-poly(galactosylated propargylglycine) (PBLG-b-PPG) have shown a specific binding to RCA_{120}.[20] In this study, the changes in absorbance of saccharide-conjugated micelles/RCA_{120} solutions at 450 nm were first investigated. As shown in Figure 4, the results revealed that the absorbance for saccharide-conjugated micelles was much higher than that for sugar-free micelles, indicating that the significant change in turbidity for saccharide-conjugated micelles/RCA_{120} solutions. The results suggested that the galactosyl residues were present on the surface of the micelles and can mediate the interaction with the target biomolecules. Concanavalin A (Con A) lectin, which is selective for glucosyl and mannosyl residues but not for galactosyl residues,[40] was used as the control. The saccharide-conjugated micelles/Con A solutions showed no change in absorbance at 450 nm, suggesting no change in turbidity. The results signified the highly specific and noncovalent carbohydrate-lectin interactions.

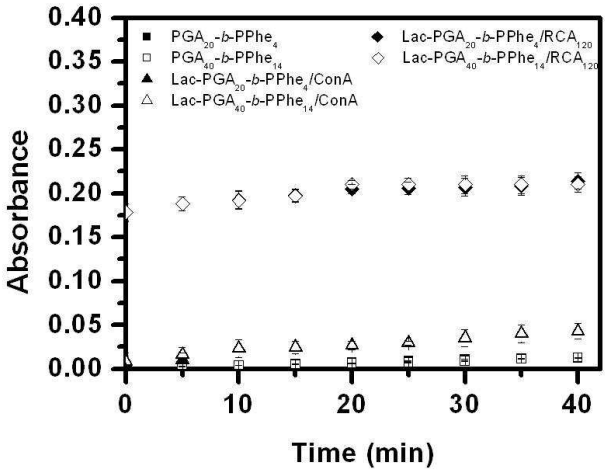

Fig. 4 Absorbance (at 450 nm) of micellar solution upon reacting with two lectins in PBS. The polymer concentration was 0.2 mg/mL.

3.5. pH-Responsive Polypeptide Micelles

In view of the micelles comprising pH-responsive PGA chains, it is expected that they exhibited stimuli-responsive property. As is known, when decreasing pH value, the PGA

chains underwent a conformational transition from coil to helix, due to the protonation of carboxyl group. The pH-dependent conformations of the polypeptide chains in saccharide-conjugated micelles and sugar-free micelles were analyzed by CD spectroscopy. At neutral condition, the far-UV CD spectra of sugar-free micelles exhibited a minimum at 197 nm and a maximum at 217 nm which are well-known doubly inflected curves, indicating that the polypeptide chains mainly adopted random coil conformation (Figure 5). This can be attributed that the confinement of polypeptides in the assembled structure can facilitate the coil-to-helix/sheet transition due to the conjugation of a PPhe block on PGA.[26, 28, 30] The incorporation of saccharides onto the micelles did not lead to the significant change of the polypeptide chain conformation at neutral condition. Upon decreasing pH to 4.7, the far-UV CD spectra exhibited a positive band at ~195 nm and a broad negative band between 200 and 230 nm, suggesting that the polypeptide chains predominantly adopted a mixture of α-helical and β-sheet conformations. The protonation of GA residues facilitated the formation of hydrogen bonding, which consequently induced the polypeptide chains undergoing the random coil-to-helix/sheet conformational changes. The results clearly demonstrated that the polypeptide chains underwent coil-to-helix/sheet transition upon decreasing pH due to the confinement of polypeptide chains in the assembled structures and the conjugation of a PPhe block, consistent with previous studies.[18, 23, 24] A similar trend was obtained when performing the CD measurements on the samples with a higher dilution factor (or a lower concentration) (see Figure S5).

The influence of pH variation on the size and zeta potential of these micelles was then investigated. For saccharide-conjugated micelles, a slight increase in particle size was observed at acidic condition (< 5.0) and the micelles were stable for days at pH 5.5~10.0 (Figure 6a). However, at pH 4.0, the particle size increased dramatically due to the formation of large aggregates (Figure S6) and the micelles precipitated out of the solution after a few minutes. In contrast, the sugar-free micelles started to aggregate and precipitate out of the

solution upon decreasing pH below 6.0. The zeta potential results showed the significant decrease in the surface negative charge of the micelles upon decreasing pH (Figure 6b). These results illustrated that the negative charge carried by PGA chains would decrease upon decreasing pH and the coil-to-helix/sheet transition would occur, leading to the decrease in hydrophilicity and solubility in solution and consequently the aggregation of the micelles. Moreover, the conjugation of water-soluble sugar moiety is able to enhance the solubility of micelles and impose steric hindrance to prevent the aggregation of micelles.

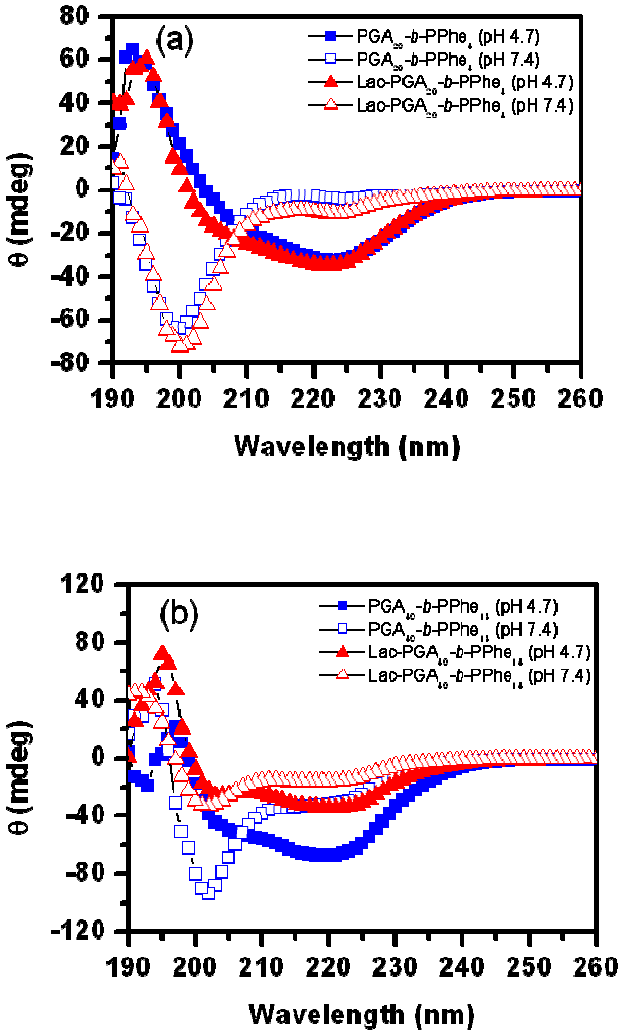

Fig. 5 CD spectra of (a) PGA_{20}-*b*-$PPhe_4$ and Lac-PGA_{20}-*b*-$PPhe_4$, and (b) PGA_{40}-*b*-$PPhe_{14}$ and Lac-PGA_{40}-*b*-$PPhe_{14}$ micelles at pH 4.7 and 7.4. The polymer concentration was 0.5 mg/mL.

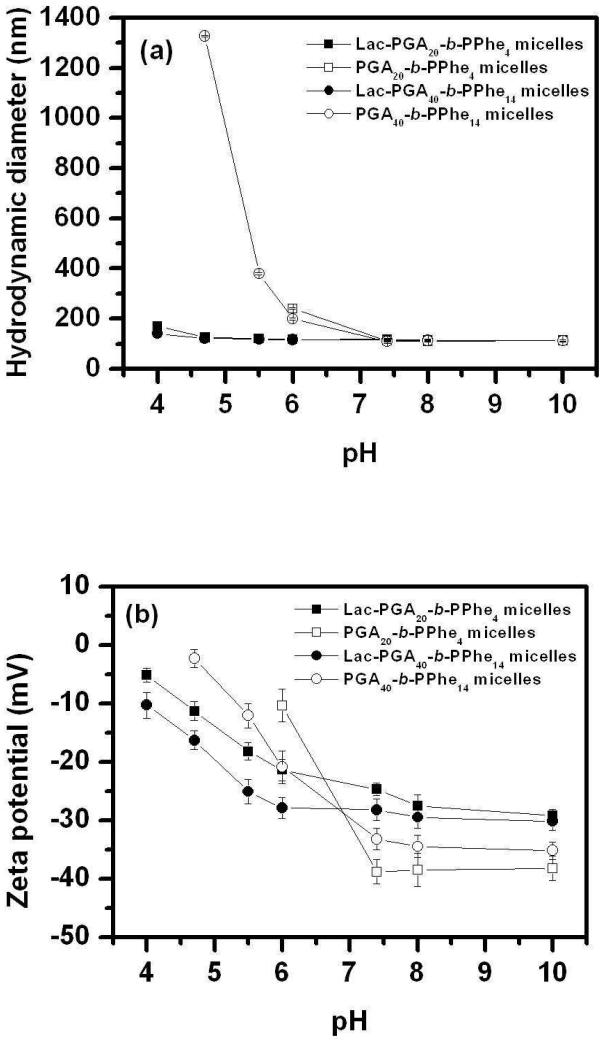

Fig. 6 (a) Hydrodynamic diameter and (b) zeta potential of micelles (2 mg/mL) as a function of pH.

3.6. In Vitro Drug Release

The anticancer drug, DOX, was chosen as a model drug and loaded into the micelles to evaluate the potentiality of these designed micelles as drug carriers. The drug was loaded via the electrostatic interaction between the DOX molecules and GA moieties. The loading content (LC) of drug for Lac-PGA_{20}-$PPhe_4$ micelles was calculated to be 6.22±1.85 wt%. Lac-PGA_{40}-b-$PPhe_{14}$ micelles exhibited relatively higher drug loading than Lac-PGA_{20}-$PPhe_4$

micelles with LC to be 7.92±0.32%. The respective sizes of DOX-loaded Lac-PGA_{20}-$PPhe_4$ and Lac-PGA_{40}-b-$PPhe_{14}$ micelles were measured to be 108.0±4.2 and 98.8±5.2 nm, which were slightly less than that of the corresponding micelles. The scattering intensity of the DOX-loaded micelles was higher than that of drug free micelles, indicating that the drug-loaded micelles become much compact structures owing to the increase in hydrophobicity by the incorporation of DOX molecules into the micelles. Moreover, the zeta potential measurements revealed that the negative charge carried by DOX-loaded micelles was reduced because that the DOX molecules (pK_a 8.3) entrapped in the micelles via electrostatic interaction between DOX and GA moieties (data not shown).

The in vitro DOX release of these DOX-loaded micelles at various pH values was investigated (Figure 7). DOX release from the micelles strongly depended on the solution pH. The release data revealed that DOX was released from the micelles faster at pH 5.5 than at pH 7.4. It can be attributed to that, with decreasing pH, the electrostatic interaction between DOX and GA moieties would be disrupted due to the decrease in the deprotonation of GA moieties, which would facilitate the escape of DOX molecules from micelles. In the control experiment, in vitro release of free drug at pH 5.5 and 7.4 was also investigated. More than 80% of drug was released within 3 h regardless the solution pH, signifying that these DOX-loaded micelles exhibited pH-sensitive behavior. Compared to Lac-PGA_{20}-b-$PPhe_4$ micelles, the release of DOX from Lac-PGA_{40}-b-$PPhe_{14}$ micelles was significantly hindered at both pH. This is mainly attributed that the Lac-PGA_{40}-$PPhe_{14}$ micelles would form more compact structure than Lac-PGA_{20}-b-$PPhe_4$ due to its relatively higher PPhe to PGA block ratio. These results revealed that the release of DOX from micelles can be tuned by the change in the solution pH and polymer composition.

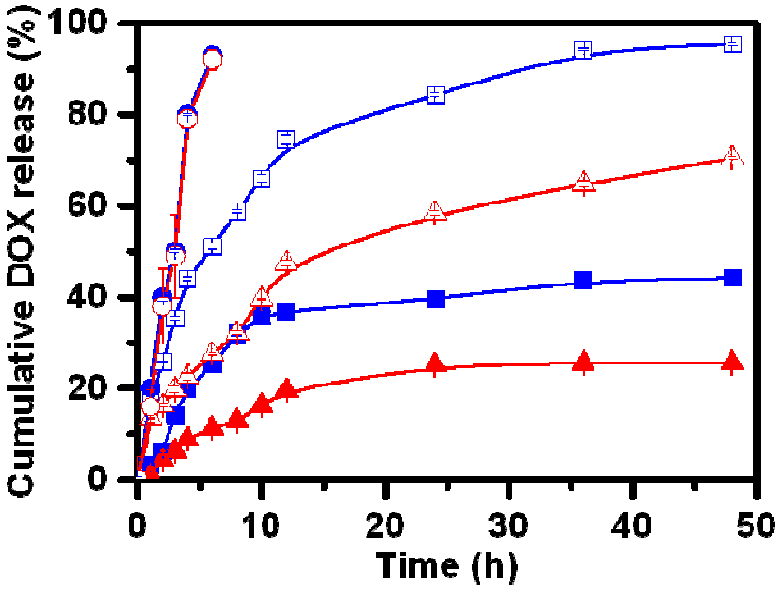

Fig. 7 Cumulative release of free DOX (circles), DOX-loaded Lac-PGA_{20}-*b*-$PPhe_4$ micelles (squares), and Lac-PGA_{40}-*b*-$PPhe_{14}$ micelles (triangles) as a function of time. The solid and open symbols denote that the DOX release was performed at pH 7.4 and 5.5, respectively.

3.7. In Vitro Cytotoxicity and Intracellular Uptake of DOX

The cytotoxicity of PGA_{20}-b-$PPhe_4$ and Lac-PGA_{20}-b-$PPhe_4$ on HepG2 cells as a function of polypeptide concentration was evaluated. As depicted in Figure S7, both PGA_{20}-b-$PPhe_4$ and Lac-PGA_{20}-b-$PPhe_4$ were found to be non-cytotoxic at the polypeptide concentration as high as 100 μg/mL, suggesting that both PGA_{20}-b-$PPhe_4$ and Lac-PGA_{20}-b-$PPhe_4$ micelles were biocompatible. Next, the cell viabilities of HepG2 cells upon exposure to the free DOX, DOX-loaded PGA_{20}-b-$PPhe_4$, and DOX-loaded Lac-PGA_{20}-b-$PPhe_4$ micelles for 24 h were determined as shown in Figure 8. It is evident that the viability of HepG2 cells was found to decrease with the increase of DOX concentration. At a low dosage (<2.0 μg/mL) of DOX, the viability by HepG2 cells treated with DOX-loaded Lac-PGA_{20}-b-$PPhe_4$ micelles was observed to be lower than that of the cells exposed to DOX-loaded PGA_{20}-b-$PPhe_4$ or free DOX ($p <$

0.05). However, at higher DOX concentrations, the free DOX and DOX-loaded micelles exhibited comparable inhibition efficiency toward HepG2 cells ($p > 0.05$).

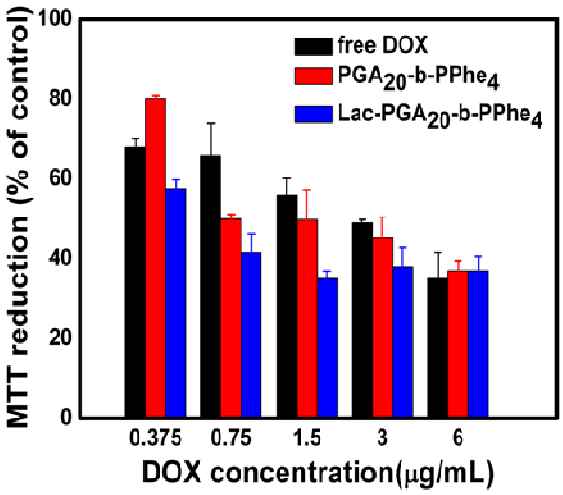

Fig. 8 Cell viabilities of free DOX (black), DOX-loaded PGA_{20}-*b*-$PPhe_4$ (red), and DOX-loaded Lac-PGA_{20}-*b*-$PPhe_4$ (blue) micelles as a function of DOX concentration.

The cellular uptake of free DOX and DOX-loaded micelles was then investigated using flow cytometry and confocal laser scanning microscopy (CLSM). The samples were HepG2 cells incubated with the free DOX, DOX-loaded PGA_{20}-*b*-$PPhe_4$, and DOX-loaded Lac-PGA_{20}-*b*-$PPhe_4$ for 1, 2, and 4 h. As shown in Figures 9 and 10, flow cytometry and CLSM analyses clearly revealed that the cellular uptake of the DOX-loaded, Lac-conjugated micelles was much higher than those of free DOX and the DOX-loaded, Lac-free micelles, evidenced by the stronger DOX fluorescence emission for the cells treated with DOX-loaded, Lac-conjugated micelles than those for the other two samples. To further confirm our cellular uptake findings, we have performed additional CLSM analyses on the samples of free DOX, DOX-loaded PGA_{20}-b-$PPhe_4$, and DOX-loaded Lac-PGA_{20}-b-$PPhe_4$ with the aid of the DOX channel and bright field settings. As can be seen in Figure S8, the merged images, which were obtained by overlaying the DOX channel and bright field ones, showed that, after incubation of the cells with DOX-loaded Lac-PGA_{20}-b-$PPhe_4$ for 1 h, the DOX red fluorescence was

detected in the cytoplasm, whereas no sign of red fluorescence was observed in the nucleus. However, significant red fluorescence was detected within the nucleus upon further incubation (e.g., 6 h). These results suggested that the uptake of DOX-loaded Lac-PGA_{20}-b-$PPhe_4$ into the HepG2 cells occurred within a short period of time, followed by the translocation of DOX into the nucleus, thereby triggering cell death.

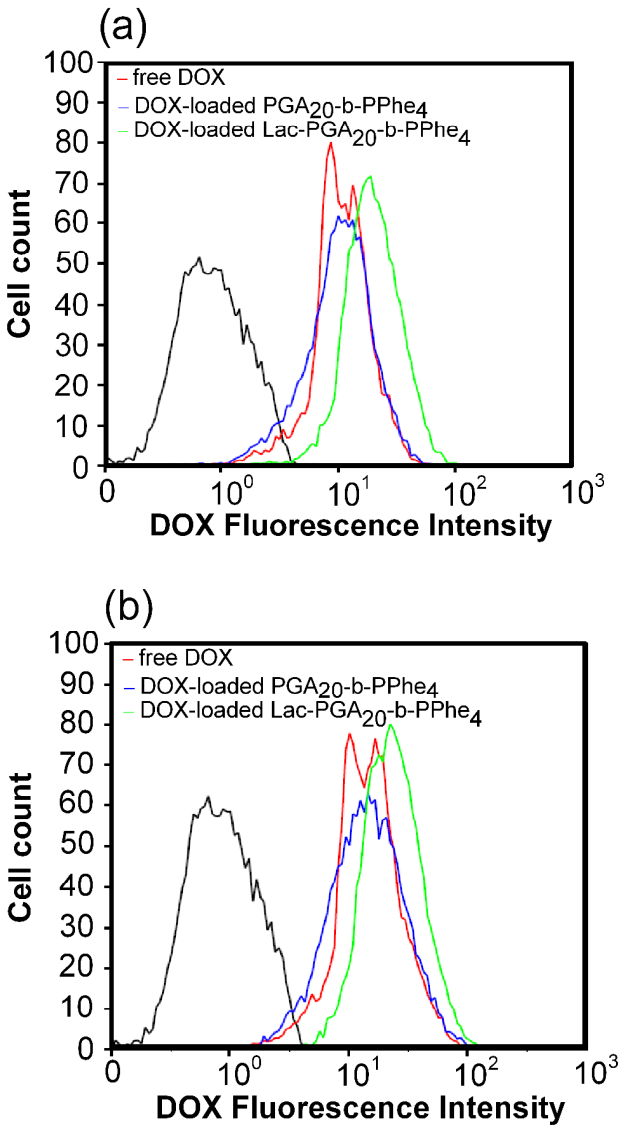

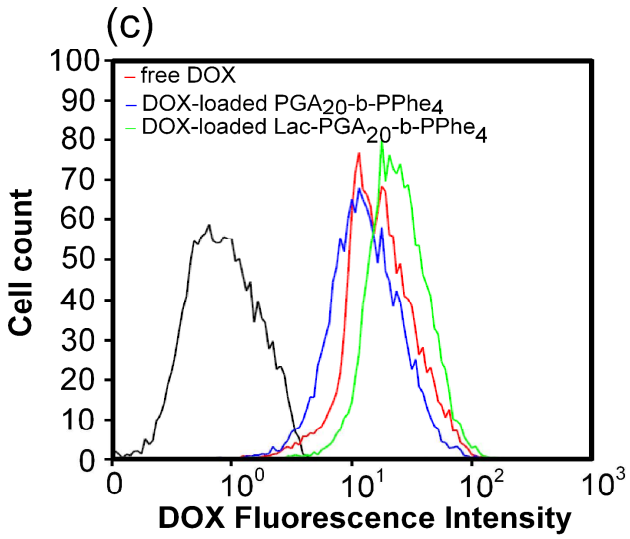

Fig. 9 DOX fluorescence intensity of HepG2 cells incubated with the free DOX (red), DOX-loaded PGA_{20}-*b*-$PPhe_4$ (blue), and DOX-loaded Lac-PGA_{20}-*b*-$PPhe_4$ (green) for (a) 1, (b) 2, and (c) 4 h measured by flow cytometry. The concentration of DOX used was 6 μg/mL.

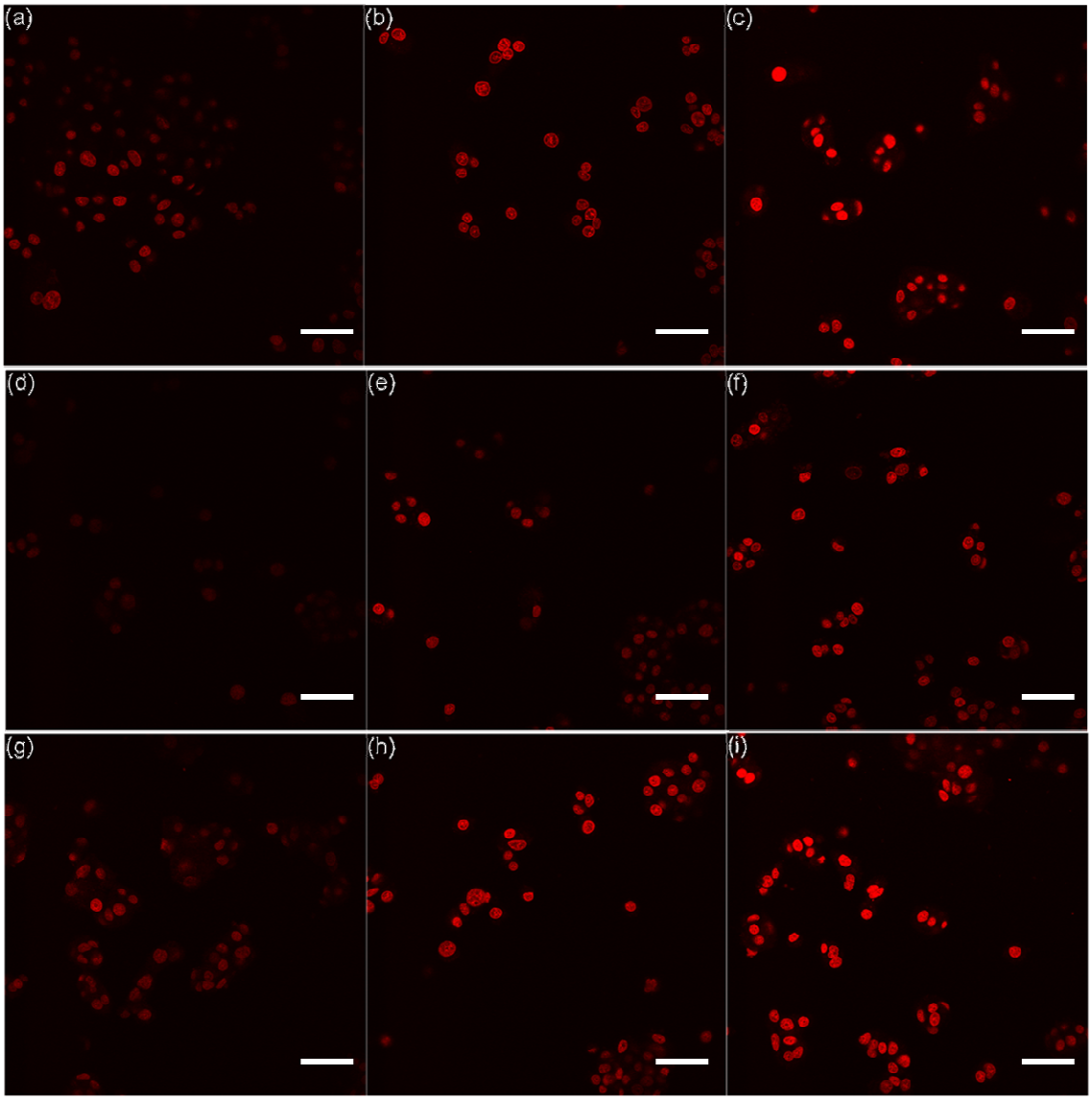

Fig. 10 CLSM images of HepG2 cells incubated with (a-c) free DOX, (d-f) DOX-loaded PGA_{20}-*b*-$PPhe_4$, and (g-i) DOX-loaded Lac-PGA_{20}-*b*-$PPhe_4$, for (a, d, g) 1, (b, e, h) 2, and (c, f, i) 4 h at pH 7.4. The concentration of DOX was 6 μg/mL. The scale bar is 50 μm.

To further elucidate the role that asialoglycoprotein receptor takes part in the increased targeted delivery/cellular uptake, a mouse fibroblast cell line L929 without expression of the asialoglycoprotein receptor was chosen as the negative control to reveal the binding specificity associated with asialoglycoprotein receptor and conjugated saccharide. The intracellular uptake behavior of free DOX or DOX-loaded micelle on L929 cells was

investigated following the analogous flow cytometric procedure. As shown in Figure S9, the cellular uptake of free DOX was found to be higher than those of the DOX-loaded micelles, evidenced by the stronger DOX fluorescence emission for the cells treated with free DOX than those treated with DOX-loaded micelles. The cellular uptake of DOX-loaded micelles on L929 cells was not as effective as that of free DOX, which was mainly transported into cells via diffusion. The results revealed that the specific interaction/binding between the Lac and asialoglycoprotein receptor might take part in the HepG2 cells, leading to the increased targeted delivery/cellular uptake.

Flow cytometry and CLSM analyses show that the DOX-loaded, Lac-conjugated micelles (6 μg/mL) can readily be recognized and uptaken by cells within a few hours, leading to the higher cellular uptake of the DOX-loaded, Lac-conjugated micelles. Rather, the *in vitro* cytoxicity experiments using MTT assay show that they exhibited comparable inhibition efficiency toward HepG2 cells at the same concentration. It is worth noting that the incubation time is 24 h. The results show that, if the incubation time is long enough, the amount of free DOX molecules transported into cells via diffusion at this high dosage could be as much as that of DOX molecules loaded in Lac-conjugated micelles uptaken by cells, which subsequently led to comparable inhibition efficiency toward HepG2 cells.

DOX is known to be transported into cells via diffusion. Given that the micelles failed to pass the cell membrane and the interaction/binding between Lac and asialoglycoprotein receptor markedly enhanced the cellular uptake of DOX-loaded micelles (see Figure S9), the uptake/internalization of DOX-loaded micelles, as observed by the flow cytometry and CLSM (see Figures 9, 10, and S8), is likely to be connected with the receptor-mediated endocytosis mechanism. Hence, we can hypothesize that the enhanced delivery and/or intracellular uptake of DOX is possibly attributed to the receptor-mediated endocytosis process, which is triggered by the specific interaction/binding between the Lac and asialoglycoprotein receptor, which is believed to be expressed on the surface of the human hepatoblastoma-derived cell

line HepG2.[41-43] The Lac-conjugated micelles can effectively bind to the cells through the asialoglycoprotein receptor-mediated recognition and subsequently the uptake of Lac-conjugated micelles was higher than that of Lac-free micelles. Higher levels of particle uptake can enhance the release of drug under the pH-sensitive condition, leading to an increase in toxicity.

4. Conclusion

In summary, we have synthesized the biocompatible PGA-*b*-PPhe and Lac-conjugated PGA-*b*-PPhe amphiphilic polypeptides, which self-assembled into spherical micelles in aqueous solution. The terminal alkyne groups of PGA segments could be conjugated with saccharide moieties via click chemistry. The conjugation of water-soluble saccharide group led to the enhancement of the particle solubility and prevention of aggregation. The fast and selective biorecognition was demonstrated by carbohydrate-lectin experiment. CD measurements revealed that the secondary conformation of PGA blocks underwent a coil-to-helix/sheet conformation transition upon decreasing the solution pH due to the confinement of the polypeptide chains. The micelles showed pH-dependent properties due to the conformational transitions of PGA chains by the changes in their ionization degree. The DOX-loaded micelles exhibited noticeable pH-sensitive behavior with accelerated DOX release at acidic condition due to the decrease in ionization degree of PGA block. The saccharide-conjugated micelles were found to effectively bind to the cells through the asialoglycoprotein receptor-mediated recognition and subsequently the higher uptake of saccharide-conjugated micelles led to the higher drug release and cytotoxicity under pH-sensitive condition. Due to the stimuli-responsiveness and molecular recognition ability of these assemblies, it can be expected that these saccharide-conjugated micelles would serve as targeted drug carriers for therapy of liver disease.

Acknowledgements

The authors thank the funding support from Ministry of Science and Technology Taiwan grants MOST 102-2221-E-006-267 and MOST 102-2221-E-002-161. This research received funding from the Headquarters of University Advancement at the National Cheng Kung University, which is sponsored by the Ministry of Education, Taiwan, ROC.

References

1. S. Förster and M. Antonietti, *Adv. Mater.* 1998, **10**, 195-217.

2. D. E. Discher and A. Eisenberg, *Science* 2002, **297**, 967-973.

3. F. Checot, S. Lecommandoux, Y. Gnanou and H.-A. Klok, *Angew. Chem. Int. Ed.* 2002, **41**, 1339-1343.

4. H. Kukula, H. Schlaad, M. Antonietti and S. Foerster, *J. Am. Chem. Soc.* 2002, **124**, 1658-1663.

5. E. G. Bellomo, M. D. Wyrsta, L. Pakstis, D. J. Pochan and T. J. Deming, *Nature Mater.* 2004, **3**, 244-248.

6. J. Sun, X. Chen, C. Deng, H. Yu, Z. Xie and X. Jing, *Langmuir* 2007, **23**, 8308-8315.

7. C. P. Leamon and J. A. Reddy, *Adv Drug Deliv Rev* 2004, **56**, 1127-1141.

8. K. Loomis, K. McNeeley and R. V. Bellamkonda, *Soft Matter* 2011, **7**, 839-856.

9. R. A. Dwek, *Chem. Rev.* 1996, **96**, 683-720.

10. A. Dove, *Nature Biotech.* 2001, **19**, 913-917.

11. D. P. Gamblin, E. M. Scanlan and B. G. Davis, *Chem. Rev.* 2009, **109**, 131-163.

12. C. Schatz and S. Lecommandoux, *Macromol. Rapid Commun.* 2010, **31**, 1664-1684.

13. K. K. Upadhyay, J.-F. Le Meins, A. Misra, P. Voisin, V. Bouchaud, E. Ibarboure, C. Schatz and S. Lecommandoux, *Biomacromolecules* 2009, **10**, 2802-2808.

14. C. Schatz, S. Louguet, J.-F. Le Meins and S. Lecommandoux, *Angew. Chem. Int. Ed.* 2009, **48**, 2572-2575.

15. J. Huang, G. Habraken, F. Audouin and A. Heise, *Macromolecules* 2010, **43**, 6050-6057.

16. J. R. Kramer and T. J. Deming, *J. Am. Chem. Soc.* 2010, **132**, 15068-15071.

17. H. Tang aand D. Zhang, *Biomacromolecules* 2010, **11**, 1585-1592.

18. A. I. Triftaridou, F. Chécot and I. Iliopoulos, *Macromol. Chem. Phys.* 2010, **211**, 768-777.

19. C. Xiao, C. Zhao, P. He, Z. Tang, X. Chen and X. Jing, *Macromol. Rapid Commun.* 2010, **31**, 991-997.

20. J. Huang, C. Bonduelle, J. Thevenot, S. Lecommandoux and A. Heise, *J. Am. Chem. Soc.* 2012, **134**, 119-122.

21. J. R. Kramer and T. J. Deming, *J. Am. Chem. Soc.* 2012, **134**, 4112-4115.

22. K. S. Krannig and H. Schlaad, *J. Am. Chem. Soc.* 2012, **134**, 18542-18545.

23. P. Wu, A. K. Feldman, A. K. Nugent, C. J. Hawker, A. Scheel, B. Voit, J. Pyun, J. M. Frechet, K. B. Sharpless and V. V. Fokin, *Angew. Chem. Int. Ed.* 2004, **43**, 3928-3932.

24. M. Malkoch, K. Schleicher, E. Drockenmuller, C. J. Hawker, T. P. Russell, P. Wu and V. V. Fokin, *Macromolecules* 2005, **38**, 3663-3678.

25. J. Gaspard, J. A. Silas, D. F. Shantz and J.-S. Jan, *Supramol. Chem.* 2010, **22**, 178-185.

26. Y.-C. Huang, M. Arham and J.-S. Jan, *Soft Matter* 2011, **7**, 3975-3983.

27. Y.-C. Huang, Y.-S. Yang, T.-Y. Lai and J.-S. Jan, *Polymer* 2012, **53**, 913-922.

28. Y.-C. Huang, M. Arham and J.-S. Jan, *Euro. Polym. J.* 2013, **49**, 726-737.

29. Y.-C. Huang and J.-S. Jan, *Polymer* 2014, **55**, 540-549.

30. B.-Y. Chen, Y.-F. Huang, Y.-C. Huang, T.-C. Wen and J.-S. Jan, *ACS Macro Lett.* 2014, **3**, 220-223.

31. Y.-F. Huang, S.-C. Lu, Y.-C. Huang and J.-S. Jan, *Small* 2014, **10**, 1939-1944.

32. L. Li, H. Wang, Z. Y. Ong, K. Xu, P. L. R. Ee, S. Zheng, J. L. Hedrick and Y.-Y.Yang, *Nano Today* 2010, **5**, 296-312.

33. C. He, X. Zhuang, Z. Tang, H. Tian and X. Chen, *Adv. Healthc. Mater.* 2012, **1**, 48-78.

34. N. T. Zaman, Y.-Y. Yang and J. Y. Ying, *Nano Today* 2010, **5**, 9-14.

35. R. Narain and S. P. Armes, *Biomacromolecules* 2003, **4**, 1746-1758.

36. T. J. Deming, *Prog. Polym. Sci.* 2007, **32**, 858-875.

37. H. R. Kricheldorf and D. Muller, *Macromolecules* 1983, **16**, 615-623.

38. F. Meng, Z. Zhong and J. Feijen, *Biomacromolecules* 2009, **10**, 197-209.

39. J. E. Hein and V. V. Fokin, *Chem. Soc. Rev.* 2010, **39**, 1302-1315.

40. M. Ambrosi, N. R. Cameron and B. G. Davis, *Org. Biomol. Chem.* 2005, **3**, 1593-1608.

41. K. Jain, P. Kesharwani, U. Gupta and N. K. Jain, *Biomaterials* 2012, **33**, 4166-4186.

42. A. Lin, Y. Liu, Y. Huang, J. Sun, Z. Wu, X. Zhang and Q. Ping, *Int. J. Pharm.* 2008, **359**, 247-253.

43. H. Zhang, Y. Ma and X. L. Sun, *Med. Res. Rev.* 2010, **30**, 270-289.

The table of contents entry

Cell-targeted, pH-sensitive saccharide-conjugated micelles exhibited higher cell uptake led to higher drug release and cytotoxicity under pH-sensitive condition.

TOC figure